Multipass acoustically open photoacoustic detector for trace gas measurements

András Miklós, Shan-Chuang Pei, and A. H. Kung

What we believe to be a novel multipass, acoustically open photoacoustic detector designed for fast-response, high-sensitivity detection of trace gases and pollutants in the atmosphere is demonstrated. The acoustic pulses generated by the absorption of the light pulses of a tunable optical parametric oscillator by target molecules are detected by an ultrasonic sensor at 40 kHz. The photoacoustic signal is enhanced by an optical multipass arrangement and by concentration of the acoustic energy to the surface of the ultrasonic sensor. The detection sensitivity, estimated from CO_2 measurements around a 2 μm wavelength, is $\sim 3.3 \times 10^{-9}$ W cm^{-1}. © 2006 Optical Society of America

OCIS codes: 280.3420, 300.6430, 280.1120, 190.4970.

1. Introduction

Photoacoustic detection of trace concentrations of gases is one of the most sensitive techniques of infrared absorption spectroscopy.[1] High-sensitivity photoacoustic detectors apply an acoustic resonator for the amplification of the weak photoacoustic signal.[2–4] They are often equipped with acoustic filters for suppressing noise generated by window absorption. These photoacoustic detectors are often used in either the stopped-flow mode or the flow-through mode. In the first case the gas flow is interrupted for the time of the measurement. This type of photoacoustic detector works in a cyclical manner, i.e., each measurement consists of three steps (filling the sample gas, measuring the photoacoustic signal, and evacuating the photoacoustic detector), and the cycle is repeated regularly when trace gas concentration changes have to be monitored.

In the second case the gas to be measured flows continuously through the photoacoustic detector. A few of these detectors were also referred to as an open photoacoustic cell[5] or a windowless photoacoustic cell.[6,7] These detectors are open for the flow, but they are acoustically closed for the sound wave generated in the resonator. To obtain high acoustic amplification in the resonator, the acoustic reflection coefficient has to be high at the open apertures of the resonator. Therefore the resonators are terminated by high acoustic impedances provided by acoustic filters. This solution also protects the acoustic resonator against the outside noise.

True free-field photoacoustic measurements have also been published.[8–10] The photoacoustic signal generated by the absorption of pulses from a powerful CO_2 laser in a liquid layer adsorbed on a solid surface was measured at a distance of a few centimeters by a microphone.[8] In a recent work[9] the distance of sound detection was increased to ~10 m by using a parabolic mirror to concentrate the acoustic energy onto the membrane of the microphone.

In another open-air application, sound signals produced by laser absorption due to SF_6 leakage were detected[10] by a microphone. Since the laser light was completely absorbed by the SF_6 in less than a 1 mm distance, the sound source could be regarded as a point source emitting an outgoing spherical acoustic wave with a $1/r^2$ spatial distribution of the sound power. Therefore the sound pressure was significantly reduced between the source and the microphone.

In the open-air measurements, the acoustic noise from the environment was the main interference factor. To obtain measurable acoustic signals, these experiments were performed using high laser pulse

A. Miklós (andreas.miklos@urz.uni-heidelberg.de) is with the Institute of Physical Chemistry, University of Heidelberg, Heidelberg, Germany. S.-C. Pei and A. H. Kung (akung@pub.iams.sinica.edu.tw) are with the Institute of Atomic and Molecular Sciences, Academic Sinica, Taipei, Taiwan, Republic of China. A. H. Kung is also with the Department of Photonics and Institute of Electro-optical Engineering, National Chiao Tung University, Hsinchu, Taiwan, Republic of China.

Received 6 June 2005; accepted 28 October 2005; posted 10 November 2005 (Doc. ID 62580).

0003-6935/06/112529-06$15.00/0

energy and strong gas absorption. Moreover, time gating or convolution techniques had to be used to suppress the acoustic noise.

In this paper we present a novel acoustically open photoacoustic detector, which can be used with pulsed laser sources having weak or medium pulse energy. This detector is designed for high-sensitivity monitoring of trace gases and pollutants in an open atmosphere. By employing high harmonic detection, the acoustic noise from the background environment is effectively eliminated.

2. Concept of the Present Detector

Some of the most important light sources for absorption spectroscopy are tunable IR solid-state lasers, such as quantum-cascade lasers, diode lasers, and optical parametric oscillators (OPOs). Many of these lasers work well in the pulsed mode, emitting nanosecond pulses at a kilohertz to megahertz repetition rate.

Consider a pulsed solid-state laser that emits light pulses with a 10–50 ns duration. The time profile of the laser pulse may be approximated by a Gaussian. The absorption of the laser pulse by a gas produces an acoustic signal whose time profile corresponds to the time derivative of the light pulse[11]; i.e., a unipolar laser pulse produces a bipolar acoustic pulse with essentially the same time duration. Since such bipolar acoustic pulses are produced everywhere in the cylindrical volume occupied by a collimated laser beam, the total duration of an acoustic pulse propagating outward from the cylindrical laser beam is proportional to the transit time of the acoustic pulse across the diameter of the laser beam. Assuming a beam diameter of 3 mm and an acoustic velocity in free air of 331 m/s, the duration of the acoustic pulse can be estimated as ~9 μs. The frequency spectrum of the bipolar acoustic pulse consists of frequency components whose amplitudes form an envelope that is close to a Gaussian peaked around 110 kHz, corresponding to a peak acoustic wavelength of around 3 mm.

In conventional photoacoustic detection, these primary acoustic pulses will excite the modes of an acoustic resonator. A single acoustic pulse, because of its broad spectrum, will generate several eigenmodes in the resonator, resulting in a complicated ringing signal. Single-mode excitation could be obtained by using a high-Q acoustic resonator with carefully designed excitation geometry and microphone position. In this case the light pulse generates a slowly decaying sine signal whose initial amplitude can be used as a quantitative measure of the absorption.[11]

Pulsed lasers that emit a periodic pulse train can be used with a resonant photoacoustic detector whose resonance frequency is close to the repetition frequency of the laser. After a short transient period a steady-state oscillation will be reached, and the microphone detects this oscillation as a signal at the repetition frequency, usually in the low kilohertz range. This technique was used successfully in measurements with a multi-kilohertz tunable optical parametric oscillation source.[12–14]

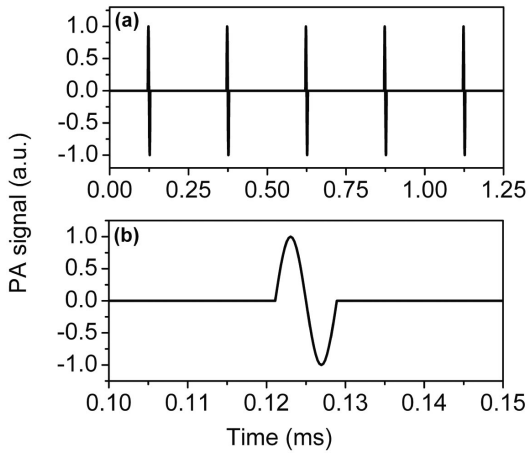

Fig. 1. Periodic train of primary acoustic pulses generated by the absorption of a 3 mm diameter beam of a pulsed laser with 4000 Hz repetition frequency. (a) Pulse train and (b) a single pulse in the train. PA, photoacoustic.

However, only a small portion of the available acoustic energy is utilized by such a detection technique. Assume that the primary acoustic signal is a periodic train of 10 μs bipolar acoustic pulses (modeled by a single period of a sine function) with a repetition rate of 4 kHz (see Fig. 1). The frequency spectrum of this signal contains components at the harmonics of the repetition rate of 4 kHz, and the amplitude of the harmonics maximizes near 100 kHz, the inverse value of the acoustic pulse duration of 10 μs. The amplitude at the peak frequency component is ~17 times higher than at the fundamental frequency (see Fig. 2).

Therefore when the above train of laser pulses is used to excite acoustic pulses in a free field, the best sensitivity is obtained if the sensor or microphone used has its peak sensitivity close to the peak of the spectral envelope, which is in the ultrasonic region. An ultrasonic sensor with resonant characteristics such that one of the harmonics of the acoustic spec-

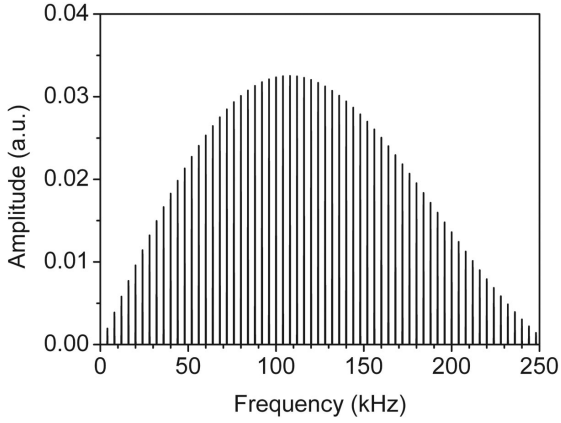

Fig. 2. Frequency spectrum given by the Fourier transform of the time signal shown in Fig. 1.

trum overlaps with the resonance peak of the sensor will be the best choice. In this case the sensor will respond at its resonant frequency, and the periodic excitation will result in a strong oscillation in the sensor. That is, the photoacoustic signal will be similar to that obtained in a resonant photoacoustic cell, but the role of the acoustic resonator is now played by the resonant ultrasonic detector. An acoustically open detector measures the primary photoacoustic signal in open air. Since all acoustic noise can freely penetrate into the detector, this device needs to function in a noisy environment. Therefore it is necessary to design a detector that will enhance the signal while discriminating against the unwanted noise.

This goal is achieved by using an optical multipass arrangement for the generation of the photoacoustic pulses, applying acoustic mirrors to concentrate the acoustic energy into a focal point and using a resonant ultrasonic sensor located at the focal region. We note that using the resonance enhancement in a high-frequency detector has been demonstrated with a quartz-crystal tuning fork that has a Q of 8000.[15] Here we show that an ultrasonic detector with a multipass arrangement could produce a similar sensitivity although it has a lower Q factor. Furthermore the ultrasonic detector is easier to align because it has a larger sensing surface. The details of the system are given in Section 3.

3. Multipass Acoustically Open Photoacoustic Detector

The multipass acoustically open photoacoustic detector[16] (MOPAD) consists of two acoustic reflectors, a plane one and a parabolic one, positioned parallel to each other, as shown in Fig. 3. The reflectors are made of Al with a polished metal surface. The parabolic reflector has a diameter of 80 mm and a focal length of 25 mm.

A laser beam is reflected back and forth between two parallel gold-coated optical mirrors to trace out a plane that is parallel to the acoustic mirrors and located 5 mm above the parabolic mirror. A typical alignment with ten passes is shown in Fig. 4. The laser beam at each pass generates an outgoing cylindrical sound wavefront. The envelopes of these wavefronts approximate two planes: One propagates toward the parabolic mirror and the other one toward the plane acoustic mirror. A small portion of the acoustic energy is lost through the open sides of the detector, but the main portion remains inside. The distance between the plane of excitation and the plane acoustic mirror is adjusted to one half of the acoustic wavelength determined by the inverse of the repetition frequency of the laser. Thus the plane wave reflected from the plane acoustic mirror will arrive back to the excitation plane at the moment when the next acoustic pulse is generated. The combined direct and reflected wavefronts propagate toward the parabolic mirror and will be focused to a point where the ultrasonic sensor is located. The ultrasonic sensor used in the experiment was a muRata sensor of type MA40B8R with a resonant response centered at 40 kHz. The directivity of the sensor is quite high, the -6 dB points (half-pressure value compared to the axis) are at $\pm 20°$, and the response for signals coming from the side at 90° is more than 30 dB weaker than the axial response.

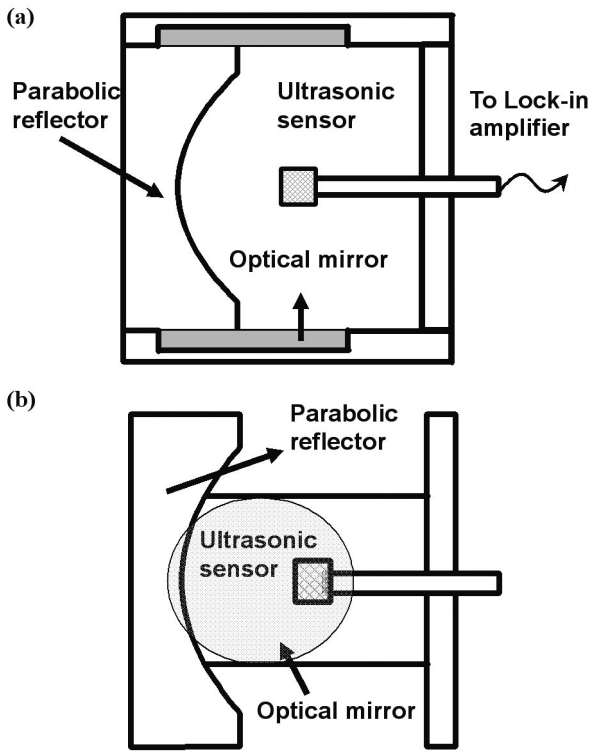

Fig. 3. Schematic views of the MOPAD: (a) the plane of the drawing is normal to the plane of the optical mirrors and contains the acoustic axis, and (b) the plane of the drawing is parallel to the optical mirrors and contains the acoustic axis.

The diameter d of the focal area is determined by the diffraction formula $d = 2.44 \times (f\lambda/D)$, where f, λ, and D are the focal length, the acoustic wavelength, and the diameter of the mirror, respectively. The acoustic wavelength here is that of the primary acoustic wave, which is approximately the same as the diameter of the laser beam. Taking $\lambda = 3$ mm, $f = 25$ mm, and $D = 80$ mm, the diameter of the focal spot can be calculated as $d = 2.3$ mm, which is much

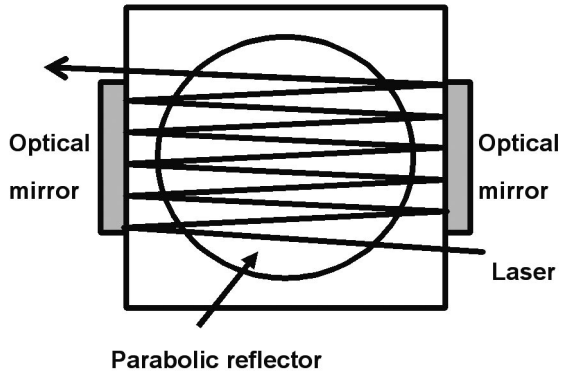

Fig. 4. View of the MOPAD showing the path of the multiple passes of the laser beam inside the detector.

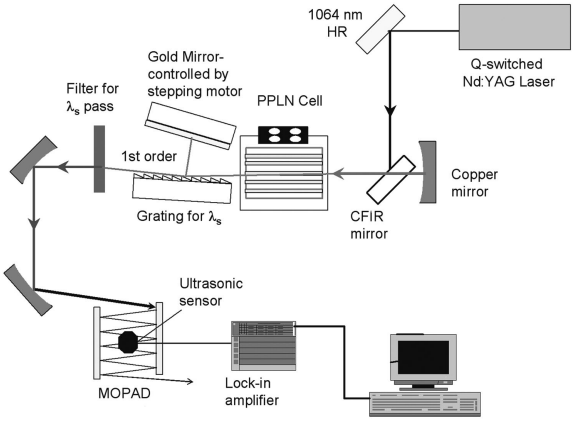

Fig. 5. Schematic diagram of the OPO and MOPAD measurement setup. HR, high reflectance; PPLN, periodically poled lithium niobate; CFIR, infrared-grade calcium fluoride.

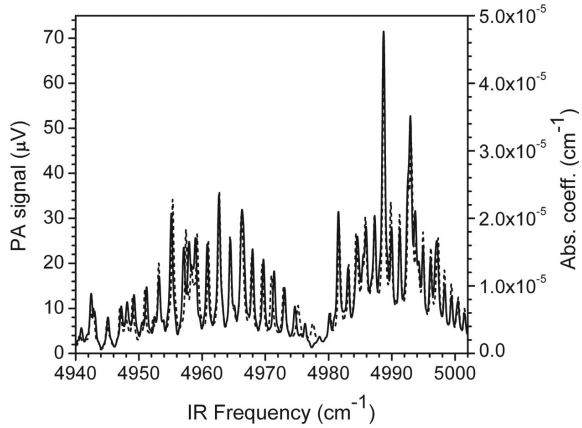

Fig. 6. Measured (dotted curve) and simulated (solid curve) photoacoustic spectra of CO_2 in ambient air in the 2 μm wavelength region. The left axis is for the measured data. PA, photoacoustic.

smaller than the ~10 mm diameter of the ultrasonic sensor. Thus all the reflected acoustic energy is concentrated within the sensing area of the detector.

The effectiveness of the energy concentration can be estimated as follows: Two plane acoustic wavefronts, a direct one and a reflected one, are concentrated simultaneously to a focal area of ~4.1 mm^2 ($\pi d^2/4$). The area of each wavefront can be estimated (see Fig. 4) as 50 mm × 70 mm = 3500 mm^2 so that the concentration factor is 7000 mm^2/4.1 mm^2 ~ 1700. This value, however, is not realistic, because only the area covered by the laser beams emits sound. The emitting surface can be estimated as 70 mm × 3 mm for each beam. Thus the total emitting surface is ~2100 mm^2 for the ten beams and 4200 mm^2 taking into account both the direct and the reflected waves. Since the primary acoustic wave is cylindrical, only the component of the primary wave that propagates in a direction parallel to the normal of the plane can be counted. This brings a factor of $2/\pi$ (the average of the integral of the cosine function from $-\pi/2$ to $\pi/2$) to yield a realistic concentration factor of $(2/\pi) \times 4200/4.1 \sim 650$ for this open photoacoustic detector design.

4. Experiment and Results

To demonstrate the utility of the MOPAD, we measured the absorption spectrum of atmospheric CO_2 in the environment of our laboratory. Figure 5 is a schematic diagram of the setup for the measurement. The IR light source was a grazing-incidence OPO based on quasi-phase-matched periodically poled $LiNbO_3$ pumped by a commercial laser-diode-pumped acousto-optic *Q*-switched Nd:YAG laser.[17] The source was operated at ~4 kHz with a pulse duration of 21 ns. The IR output was tuned to around 2 μm.

After passing through the filter, the IR beam was aligned to make ten passes through the open cell of the MOPAD. An ultrasonic sensor was located at the center of the plane carved out by the laser beam.

The photoacoustic signal detected by the ultrasonic sensor was fed into a lock-in amplifier (Stanford Research SR830 DSP), which was triggered at the laser repetition rate. The time constant of the lock-in amplifier was set to 0.3 s.

The lock-in amplifier was set for harmonic detection, and the harmonic number and the laser repetition rate were adjusted to maximize the photoacoustic signal. This condition was achieved at a 4.11 kHz repetition rate and harmonic number 10. Notice that the 41.1 kHz frequency is still far from the optimal detection range around 100 kHz. A factor of 2–3 improvement in the sensitivity could be expected with a sensor matched to the optimal frequency range of the photoacoustic signal.

The experiment was controlled by a LabVIEW code. Photoacoustic spectra were taken by scanning the OPO by means of a stepping motor through a wavelength range where CO_2 absorbs. The lock-in output signal, output phase, and laser power were recorded at each wavelength step. The recorded data were evaluated by using ORIGIN software.

The photoacoustic spectrum of CO_2 was measured around 2 μm, where CO_2 has a vibrational–rotational band structure. HITRAN spectra for different water and CO_2 concentrations were convolved with the IR line-shape function and were compared with the measured photoacoustic spectrum. The best agreement was found at 500 parts per million CO_2 and 1.7% water concentrations, which are reasonable values inside a laboratory where several people were working. The measured and simulated spectra are shown in Fig. 6. The elevated baseline in the CO_2 spectrum is a consequence of the finite OPO line shape. The irregularities in the measured CO_2 absorption band structure are due to interference of the water absorption lines.

It is not easy to determine the absolute sensitivity of the novel MOPAD system. The most serious problems are the absorption due to the presence of unknown air pollutants and spurious photoacoustic signals generated everywhere along the laser beam. Both phenomena could result in an increase of the background signal in the MOPAD cell. It was found,

however, that the background signal measured by blocking the laser beam in front of the cell decreased to the level of the acoustic–electronic noise of ~40 nV measured by shutting off the pump laser in some wavelength regions. This average noise figure of 40 nV allowed us to make an estimation of the sensitivity of the open cell, using the result of the CO_2 measurement. The signal at the frequency of 4964.4 cm^{-1} whose peak corresponds to 25.8 μV was selected in Fig. 6 and compared with the absorption coefficient $\alpha = 1.67 \times 10^{-5}\ cm^{-1}$ from HITRAN. The minimal detectable absorption coefficient at a signal-to-noise ratio (SNR) of 1 is estimated as $\alpha_{min} = (0.04\ \mu V/25.8\ \mu V) \times 1.67 \times 10^{-5}\ cm^{-1} = 2.6 \times 10^{-8}\ cm^{-1}$. Taking into account the 126 mW power of the OPO at that wavelength, a sensitivity of $S = 3.3 \times 10^{-9}\ W\ cm^{-1}$ is estimated for the MOPAD. This value is only approximately three times smaller than the sensitivity value ($S = 1 \times 10^{-9}\ W\ cm^{-1}$) of the significantly more complex enclosed differential photoacoustic cell[18,19] with an acoustic resonator.

An alternative way to determine the sensitivity is to compare the signals detected by the open cell with those by a calibrated closed differential cell. We mounted a differential cell used in a previous experiment[13] in front of the open cell and aligned the laser beam first through the differential cell and then the open cell. Ambient air was pulled through the differential cell with a peristaltic pump. The noise and pressure fluctuations produced by this pump were damped by using an ~1 m long plastic tubing between the differential cell and the pump. The acoustic background noise measured when the OPO was turned off was the same with and without the air pumping.

The average value of the photoacoustic signal measured by tuning the OPO to the peak at 4964.4 cm^{-1} was 557 μV for the differential cell and 22.1 μV for the open cell. The difference in magnitude of the signal is mainly due to the higher sensitivity of the electret microphone compared with the ultrasound sensor. However, the noise was also higher: ~0.270 μV for the differential cell compared with the 0.040 μV noise of the open cell. Thus the overall SNR of the differential cell (SNR of 2060) was approximately only a factor of 3.7 larger than that of the open cell (SNR of 550). Since the detection sensitivity of the differential cell has been determined[13] as $S_{closed} = 1 \times 10^{-9}\ W\ cm^{-1}$, a sensitivity of $S_{open} = 3.7 \times 10^{-9}\ W\ cm^{-1}$ can be deduced for the acoustically open multipass photoacoustic detector. This value is in good agreement with that estimated from the previous paragraph.

5. Discussion

The feasibility of a novel acoustically open photoacoustic detector for trace gas detection and monitoring has been successfully demonstrated. In the new design the advantages of an optical multipass arrangement, acoustic energy concentration, and high-frequency signal detection by a resonant ultrasonic detector are combined in a compact unit, which can be used without gas sampling in free air in an arbitrarily acoustically noisy environment.

The detector can be placed in an open environment where the air or gas is to be monitored. The detector can respond to changes of the gas concentration in the environment instantaneously to within a few time constants of the measurement electronics. Because of the high detection frequency and narrow bandwidth of the MOPAD, there is almost zero acoustic noise that could disturb the signal. Therefore the noise floor of the novel detector is equivalent to or better than that of the best closed photoacoustic detectors.[18]

The amplitude of the signal for comparable absorption and laser power is smaller than that of the differential detector. This difference is a consequence of the lower sensitivity of the ultrasonic sensor (typically ~1 mV/Pa) in comparison with the sensitivity of the miniature electret microphones (~100 mV/Pa).

There are several possibilities to improve the overall detection sensitivity of the MOPAD. First, impedance matching of the ultrasonic sensor to the input channel of the lock-in amplifier could be better. Similarly, the acoustic impedance mismatch between that of air and the sensor could be reduced by applying an acoustic antireflection layer on the sensor surface. As mentioned before, a sensor with a higher resonance frequency would also be better. Finally, a smaller beam diameter and more light passes inside the detector could increase the signal. Thus the sensitivity limits achieved by acoustically closed photoacoustic detectors could be approached by the MOPAD in the next step of the development.

In ambient air there are several hundred different pollutant molecules. To facilitate their identification without a molecule-specific separation step preceding the photoacoustic measurement, and to reduce the interference of water absorption, the IR fingerprint region should be selected for the utility of this open design. In this wavelength region the characteristic absorption bands of the different molecules can be well distinguished. Simultaneous multiwavelength monitoring will provide high species selectivity.

The MOPAD could be combined with compact pulsed lasers such as the quantum-cascade lasers that work in the IR fingerprint region for trace gas sensing in open air. Such a device will be an ideal tool to monitor concentration changes of species that are unstable or tend to adsorb on surfaces, such as ozone, NO, NO_2, ammonia, water, SO_2, etc. To avoid spurious photoacoustic absorption signals from the environment, the quantum-cascade laser could be integrated with the open cell into a compact mechanical unit.

A. Miklós acknowledges the Institute of Atomic and Molecular Sciences, Academia Sinica, for supporting his stay there.

References

1. M. W. Sigrist, *Air Monitoring by Spectroscopic Techniques* (Wiley, 1994).

2. F. G. C. Bijnen, J. Reuss, and F. J. M. Harren, "Geometrical optimization of a longitudinal resonant photoacoustic cell for sensitive and fast trace gas detection," Rev. Sci. Instrum. **67,** 2914–2923 (1996).
3. A. Miklós and P. Hess, "Modulated and pulsed photoacoustics in trace gas analysis," Anal. Chem. **72,** 30A–37A (2000).
4. S. Bernegger and M. W. Sigrist, "CO-laser photoacoustic spectroscopy of gases and vapors for trace gas analysis," Infrared Phys. **30,** 375–429 (1990).
5. C. Brand, A. Winkler, P. Hess, A. Miklós, Z. Bozóki, and J. Sneider, "Pulsed-laser excitation of acoustic modes in open high-*Q* photoacoustic resonators for trace gas monitoring: results for C_2H_4," Appl. Opt. **34,** 3257–3266 (1995).
6. R. Gerlach and N. M. Amer, "Sensitive in situ trace-gas detection by photothermal deflection spectroscopy," Appl. Phys. Lett. **37,** 519–521 (1980).
7. G. Z. Angeli, A. M. Sólyom, A. Miklós, and D. D. Bicanic, "Calibration of a windowless photoacoustic cell for detection of trace gases," Anal. Chem. **64,** 155–158 (1992).
8. M. Harris, G. N. Pearson, D. V. Willets, K. Ridley, P. R. Tapster, and B. Perrett, "Pulsed indirect photoacoustic spectroscopy: application to remote detection of condensed phases," Appl. Opt. **39,** 1032–1041 (2000).
9. B. Perrett, M. Harris, G. N. Pearson, D. V. Willets, and M. C. Pitter, "Remote photoacoustic detection of liquid contamination of a surface," Appl. Opt. **42,** 4901–4908 (2003).
10. E. Huang, D. R. Rowling, T. Whelan, and J. L. Spiesberger, "High-sensitivity photoacoustic leak testing," J. Acoust. Soc. Am. **114,** 1926–1933 (2003).
11. S. Schäfer, A. Miklós, and P. Hess, "Quantitative signal analysis in pulsed resonant photoacoustics," Appl. Opt. **36,** 3202–3211 (1997).
12. G.-C. Liang, H.-H. Liu, A. H. Kung, A. Mohacsi, A. Miklos, and P. Hess, "Photoacoustic trace detection of methane using compact solid-state lasers," J. Phys. Chem. A **104,** 10179–10183 (2000).
13. A. Miklós, Ch.-H. Lim, W. W. Hsiang, G.-C. Liang, A. H. Kung, A. Schmohl, and P. Hess, "Photoacoustic measurement of methane concentration using a compact pulsed optical parametric oscillator," Appl. Opt. **41,** 2985–2993 (2002).
14. J. Ng, A. H. Kung, A. Miklós, and P. Hess, "Sensitive wavelength-modulated photoacoustic spectroscopy with a pulsed optical parametric oscillator," Opt. Lett. **29,** 1206–1208 (2004).
15. A. A. Kosterev, Yu. A. Bakhirkin, R. F. Curl, and F. K. Tittel, "Quartz-enhanced photoacoustic spectroscopy," Opt. Lett. **27,** 1902–1904 (2002).
16. A. Miklós, J. Angster, K. Sedlbauer, K. Breuer, and A. H. Kung, "Acoustically open, optically multipass, high frequency photoacoustic detector for free-field trace gas measurements," patent pending, German Patent Office, submission number 10 2005 030 151.7–52.
17. C.-S. Yu and A. H. Kung, "Grazing-incidence periodically poled $LiNbO_3$ optical parametric oscillator," J. Opt. Soc. Am. B **16,** 2233–2238 (1999).
18. A. Miklós, P. Hess, and Z. Bozoki, "Application of acoustic resonators in photoacoustic trace gas analysis and metrology," Rev. Sci. Instrum. **72,** 1937–1955 (2001).
19. A. Schmohl, A. Miklós, and P. Hess, "Detection of ammonia by photoacoustic spectroscopy with semiconductor lasers," Appl. Opt. **41,** 1815–1823 (2002).